Journal of Sound and Vibration (1999) **225**(2), 327–343
Article No. jsvi.1999.2250, available online at http://www.idealibrary.com on IDEAL®

AN ASSEMBLED PLATE ACTIVE CONTROL DAMPING SET-UP: OPTIMIZATION AND CONTROL

B. JEMAI, M. N. ICHCHOU AND L. JÉZÉQUEL

Laboratoire de Tribologie et de Dynamique des Systèmes, UMR CNRS 5513, *Ecole Centrale de Lyon, B.P.* 163, 69131 *Ecully Cedex, France*

AND

M. NOE

Centre de recherche de Hutchinson, 4512 *Chalette sur Loing, France*

(*Received* 16 *April* 1998, *and in final form* 18 *March* 1999)

This paper is concerned with active structural control by using the independent modal strategy control (IMSC). Distributed sensors and actuators are of PZT ceramics or PVDF polymer. The structure under study consists of three shaped plates which are soldered. To build the control loop, the modal filtering concept is introduced in order to extract in real time the modal variables of the controlled modes. This is possible by introducing a numerical method to optimize shape and location of the sensors and actuators on the structure and to minimize the effects of the unwanted modes. Experimental identification of the structure model is then handled and compared to that obtained from a finite element analysis. The impedance problem between sensors and the acquisition system is solved and the output signal, in staircase form, of the DSP card is smoothed by analog filtering. Two kinds of modal control (the IMSControl and Time-Sharing) are tested. Both of them are stable and robust and give often to the damping ratios structure studied, ten times greater.

1. INTRODUCTION

The control of distributed-parameter systems has received a great deal of attention in recent years. In particular, Meirovitch [1–4] has adapted the independent modal space control theory to such systems. This method is attractive because it is simple in theory, but the major difficulty is how to implement it in practice.

Meirovitch [1] has proposed a method to implement the controller. He has introduced the notion of a modal filter by using a set of discrete sensors which measure displacements at different points of the structure. Thus, one can interpolate the displacement on the whole domain of the structure and then project it on the modal basis to obtain the modal variables. He proposed to use as many actuators as the number of modes to control without any optimization. Linderberg [5] has proposed later to reduce the actuators' number and introduced then the pseudoinverse of actuation matrix which unfortunately caused the spillover phenomena. He proposed an optimization method to reduce the effect of spillover.

Nowadays smart materials such as piezoceramics are often used in control. They are of great interest, because they are easy to handle and activated with a simple voltage generator.

This paper presents a study of all steps of implementation of the IMSControl on a complex structure when using piezoceramics sensors and actuators. It is assumed to work in the 0–100 Hz frequency band, with the construction of a modal filter optimized by selection of the sensors locations. Since it is aimed to control the first five modes, five sensors optimally located used to extract the first five modal variables. Two optimized actuators are used to control in real time one mode. In this way, one may reduce considerably the spillover problems. To demonstrate the advantages of optimal design, an experimental study has been conducted. Some technical solutions are proposed to make impedance adaptation and to smooth some signals.

2. MODAL CONTROL STRATEGY

In the case of light internal damping, the discrete equations of the system's motion are

$$Kw + C\dot{w} + M\ddot{w} = Lu + Df, \tag{1}$$

where w is the displacements, u the control command, f the external excitation, and M, C and K are mass, stiffness and damping matrices. L and D are location matrices of control command and external driving. Let $\phi_1, \phi_2, \dots, \phi_N$ be the N elements of the modal basis of system (1), so one can write the displacement w as

$$w = \sum_{k=1}^{N} \phi_k q_k = \Phi^{\mathrm{t}} q \tag{2}$$

where q denotes the modal co-ordinate vector. If one considers Basil's hypothesis one can write

$$\ddot{q} + c\dot{q} + \omega^2 q = \Phi^{\mathrm{t}} Lu + \Phi^{\mathrm{t}} Df, \tag{3}$$

where ω^2 is a diagonal matrix containing the squares of the natural frequencies ($\omega^2 = \Phi^{\mathrm{t}} K \Phi$) and c is also a diagonal matrix defined by $c = \Phi^{\mathrm{t}} C \Phi$. In equation (3), the term u of control command will couple all modes of the system because it depends on all the modal variables. As it is supposed that in the modal control, the command depends only on the modal variables of the mode to be controlled, so one has to introduce a modal filter of actuation K^a that satisfies

$$\Phi^{\mathrm{t}} L K^a = I, \tag{4}$$

where I is an identity matrix.

One can now introduce W_k the state vector of the mode k, and write easily the state equation of the mode k,

$$\dot{W}_k = A_k W_k + u_k + f_k, \tag{5}$$

where

$$W_k = \begin{pmatrix} q_k \\ \dot{q}_k \end{pmatrix}, \qquad A_k = \begin{bmatrix} 0 & 1 \\ -\omega_k^2 & -c_k \end{bmatrix}$$

and $c_k = \xi_k \omega_k^2$ $[u_1, \ldots, u_N]^{\mathrm{t}} = \Phi^{\mathrm{t}} Lu$ and $[f_1, \ldots, f_N]^{\mathrm{t}} = \Phi^{\mathrm{t}} Df$.

To find the control command, one has to minimize a performance index (PI) with respect to the constraint of equation (5). The performance index can be written as a sum of modal performance indices, because all the modes are decoupled as

$$PI = \sum_{k=1}^{N} PI_k, \tag{6}$$

where

$$PI_k = (W_k(t_f) - \hat{W}_k)^{\mathrm{t}} H_k (W_k(t_f) - \hat{W}_k) + \int_{t_0}^{t_f} \begin{pmatrix} W_k \\ u_k \end{pmatrix}^{\mathrm{t}} \begin{pmatrix} Q_k & 0 \\ 0 & R_k \end{pmatrix} \begin{pmatrix} W_k \\ u_k \end{pmatrix} \mathrm{d}t. \tag{7}$$

In this equation, $\hat{W}_k$ is the final state of the system to reach with control, H_k and Q_k are a 2×2 weighting matrices and R_k is a control weighting matrix. In this study, it is convenient to take $\hat{W}_k = 0$ $H_k = 0$,

$$Q_k = \begin{bmatrix} \omega_k^2 & 0 \\ 0 & 1 \end{bmatrix} \quad \text{and} \quad R_k = \alpha_k,$$

a scalar. As a result of optimization, the modal control law is in the form of a PD control operating on the modal displacement with the control gains obtained by using the linear quadratic control method with the performance index trading off the energy of the controlled mode against the energy of control input as expressed in equation (7).

As one can note, the control command is a function of modal displacements and velocities. So one needs to extract the necessary modal variables from the sensor outputs, hence the notion of modal filter matrices is introduced. If one considers the output y_i^s of the sensor i being a function of the first n modal variables, one can write

$$y_i^s = \sum_{j=1}^{n} K_{ij}^s q_j. \tag{8}$$

The superscript (s) will denote all the variables and parameters of the output sensors and the superscript (a) will denote all the variables and parameters of the actuators.

One needs then to use n sensors to construct a square and non-singular modal filter matrix, since one has to multiply the output vector $[y_1^s, \ldots, y_n^s]^{\mathrm{t}}$ by the $(K^s)^{-1}$

[where $(K^s)_{ij} = K^s_{ij}$] to obtain the modal variables q_i. Finally, one has also to construct an actuation modal filter in order to uncouple modes. The spillover phenomenon occurs when the sensor's and actuator's locations are not optimized.

3. OPTIMAL LOCATION OF PIEZOELECTRICS

Based on the work of Lee [6], it is possible to show that the voltage picked up from the kth PZT sensor which is glued on the structure can be written with respect to the notations in Figure 1 in the form

$$V^s_k = R \sum_{i=1}^{N} \frac{\partial q_i}{\partial t} K^s_{ki}, \tag{9}$$

where R is the electric resistance of measurement device,

$$K^s_{ki} = -1/2(z_3 + z_4) \iint_{Sk} \left(e_{31} \frac{\partial^2 \phi_i}{\partial^2 x} + e_{32} \frac{\partial^2 \phi_i}{\partial^2 y} \right) \mathrm{d}x\,\mathrm{d}y = \iint_{Sk} (\Lambda_i(x, y))\,\mathrm{d}x\,\mathrm{d}y, \tag{10}$$

e_{31} and e_{32} are piezoelectric constants, ϕ_i is the ith modal shape of the structure, S_k is the domain of the kth layer and $\Lambda_i(x, y)$ is the ith modal field density. For the whole set of n sensors one can write

$$V^s = (V^s_1, V^s_2, \ldots, V^s_n)^{\mathrm{t}} = RK^s \dot{Q}_{N \times 1},$$

where K^s is an $N \times 1$ matrix and $\dot{Q}_{N \times 1} = (\dot{q}_1, \dot{q}_2, \ldots, \dot{q}_N)^{\mathrm{t}}$.

As the number n of modes to control is smaller than the number N of modes kept in the structural model, one can develop the equation as

$$V^s = R[K^s(1{:}n, 1{:}n) \,|\, K^s(1{:}n, n+1{:}N)]\dot{Q}_{N \times 1}. \tag{11}$$

Multiplying equation (11) by the inverse of the matrix $RK^s(1{:}n,1{:}n)$, one obtains quantity which is a sum of two terms, such as

$$\begin{aligned} R^{-1}[K^s(1{:}n, 1{:}n)]^{-1} V^s &= I_{n \times n}(\dot{q}_i)^{\mathrm{t}}_{1 \leqslant i \leqslant n} \\ &+ [K^s(1{:}n, 1{:}n)]^{-1}[K^s(1{:}n, n+1{:}N)](\dot{q}_i)^{\mathrm{t}}_{n+1 \leqslant i \leqslant N} \end{aligned} \tag{12}$$

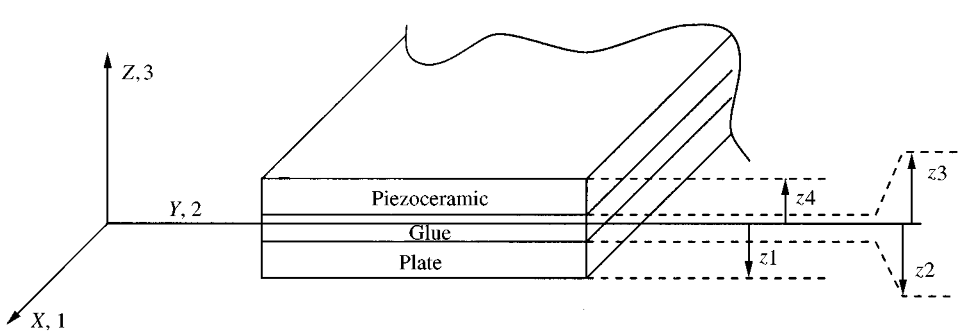

Figure 1. Piezoelectric layer glued on a structure.

The first term is the modal velocities vector of the n modes to be controlled, and the second is an error term caused by the unwanted modes. This term is causing the problem of spill-over. One can proceed to optimize shape and location of PZT layers in order to minimize the effects of the second term. If one considers the work on sensor and actuator location optimization, the matrix $K^s(1:n, 1:N)$ determines the properties of observability Gramian which measures the output energy of sensors. Indeed, Hac and Liu [7] showed that when damping is small and all natural frequencies are well spaced, this Gramian is dominated by the diagonal elements which are

$$Q_{ii} = \mathrm{diag}\left(\frac{c_{vii}}{4\xi_i\omega_i}, \frac{c_{vii}}{4\xi_i\omega_i}\right),$$

where in the case of PZT layers sensors, $c_{vii} = \sum_{k=1}^{n} K_{ki}^{s2}$. Thus, in order to guarantee under operating conditions that the contributions of individual modes 1 to n are as large as possible and the effects of residual modes are as small as possible, one has to maximize the diagonal elements 1 to n of the observability Gramian and minimize the effects of residual modes $n+1$ to N. Thus one can minimize a simplified criterion PI_k for the kth sensor as defined in reference [8]:

$$PI_k = \sum_{i=1}^{n} \frac{a_i}{K_{ki}^{s2}} + \sum_{i=1}^{N} b_i K_{ki}^{s2}. \tag{13}$$

Coefficients a_i, b_i are here to guarantee well-conditioned computations. The same kind of computation has been made for PZT layers actuators. Indeed the modal equations of a structure with a PZT layers are

$$\ddot{q}_k + 2\xi_k\omega_k\dot{q}_k + \omega_k^2 q_k = \sum_{j=1}^{p} K^a(k,j)\,V_j^a, \tag{14}$$

where p is the number of actuators on the structure and $u_k = \sum_{j=1}^{p} K^a(k,j)\,V_j^a$ is the modal driving of the actuator j on mode k. Referring to the same work of Hac and Liu [7], one can also define a controllability Gramian for the actuator. Its diagonal terms represent the modal energy control imparted into the structure by the actuators. The optimization consist of maximizing this input energy and choosing the suitable location to minimize input spill-over.

In the experimental study, as mentioned in equation (9) one is able to extract only the modal velocities with the modal filter. Moreover, one needs both modal displacement and velocities to construct the control law. It will be seen in Section 4 how to obtain these modal variables.

4. NUMERICAL OPTIMIZATION

The mechanical structure under study is a set of three rectangular plates of aluminium which are soldered and clamped on two opposite edges as shown in Figure 2. The frequency band of interest is 0–100 Hz. Thus, only the first n modes in that band are useful for the control. It was decided, to optimize n (here $n = 5$)

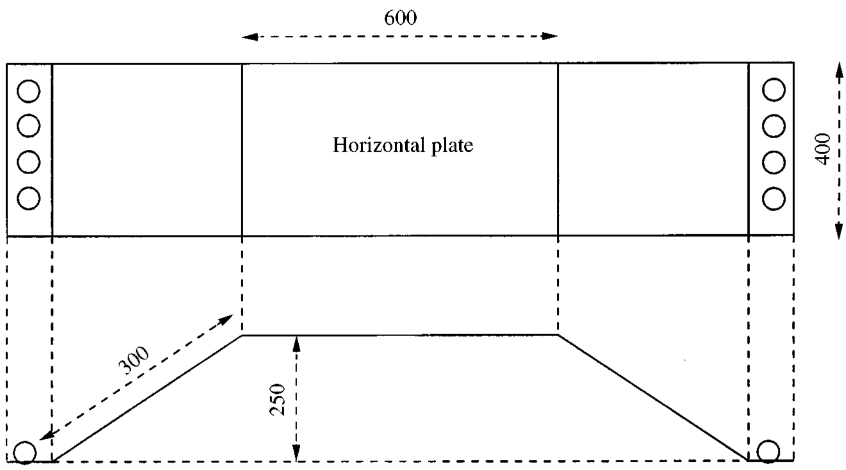

Figure 2. Mechanical structure (unit is mm).

sensors to construct the modal filter for the first five modes and to minimize at the same time the output spill-over of modes 6–8. The modal shapes corresponding to the set of eight first modes are shown in Figure 3.

The numerical steps consist of computing a polynomial function that approximates in the least-squares sense the discrete modal shape which is obtained by a finite element method. Thus, one is able to evaluate the current density on the whole structure, since this density is proportional to the second derivatives of modal shapes. Shown in Figures 5 and 4 are examples of current density for mode 3 and in Figures 6 and 7, a superposition of lines of zeros current densities of modes 6, 7 and 8. The intersections of these lines are approximately the locations of the sensors.

It is assumed that the sensor and actuator are rectangular. The criterion PI_k is a function of four variables (x, y, l, L) which determine the location and the sizes of the sensor patches. The numerical method for the optimization step consists of constructing a function $PI_k(x, y, l, L)$ and then using a Nelder-Mead Simplex method to minimize it. This method allows one to find a local minimum near the starting vector (x_0, y_0, l_0, L_0), where x_0 and y_0 are the co-ordinates of the zero current density lines of modes 6–8. Two actuators are also optimized in the same way. The results of optimization are shown in Figure 8.

A study of the effects on the modal shapes of placing the PZT layers on the structure is conducted. It justifies the assumptions that the mode shape functions are independent of adding these layers. The quality of IMSC control is related to that of modal filter. Thus, a good experimental identification of the modal filter matrix is necessary.

5. EXPERIMENTATION

The mechanical structure is shown in Figure 2. The piezoelectric layers are glued on with a M-BOND adhesive resin type AE. Figure 9 is a photo of the experimental

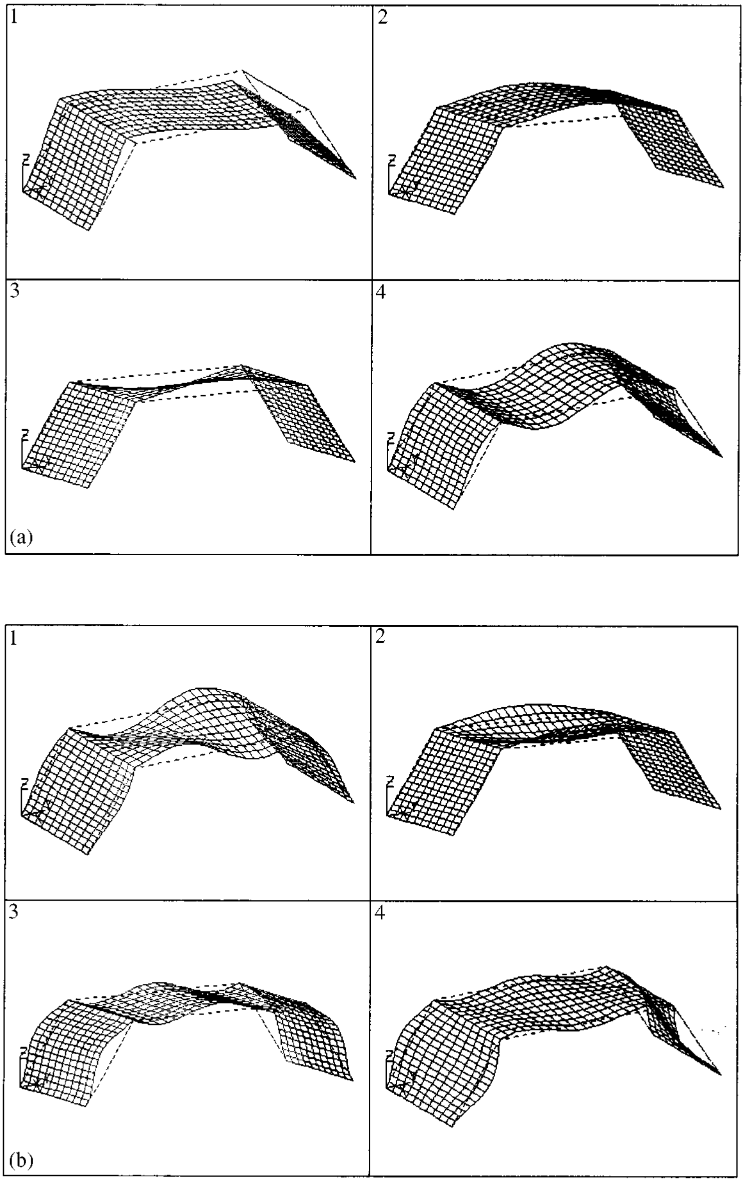

Figure 3. Modal shapes considered in modal control and optimization. (a) Modal shapes for modes 1 to 4 respectively, (b) modal shapes for modes 5 to 8 respectively.

equipment (an accelerometer, a shaker, a PC spectrum analyser HP 3566A/3567, a chock hummer used in the identification step and a board card processor Dspace DSP1002 used in control step). Before any experimental control, it was necessary to ensure a good impedance adaptation between the sensors and the material of measurement. In particular, for our experimental instrumentation if the sensors are directly connected to the board card processor Dspace DSP1002, we introduce a high-pass filter s shown in Figure 10.

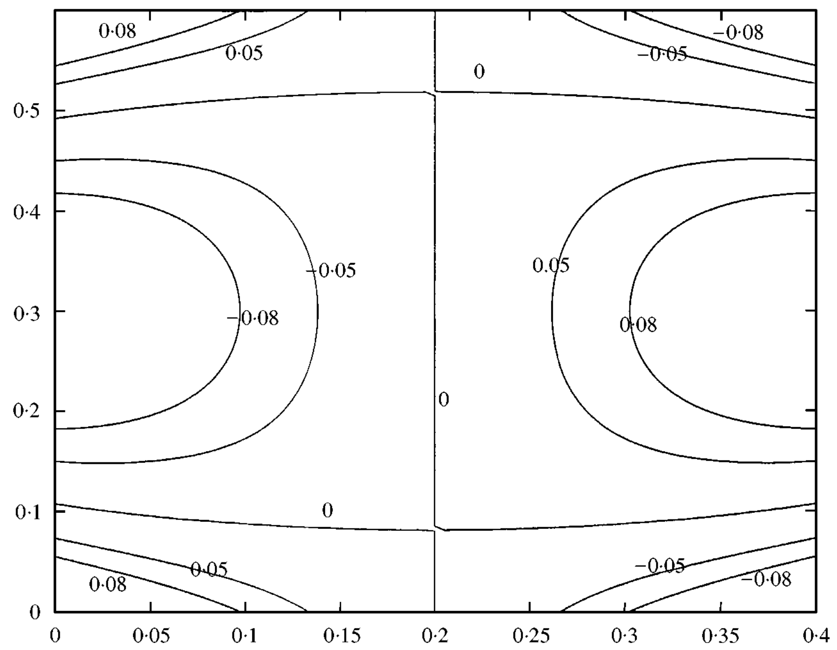

Figure 4. Example of iso-current density on the horizontal plate for mode 3.

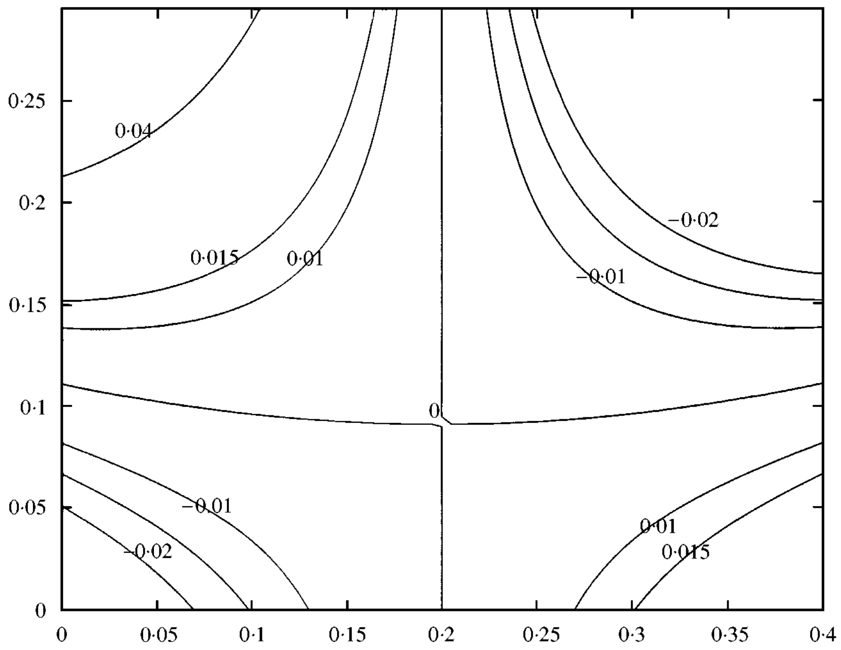

Figure 5. Example of iso-current density on the inclined plate (1 or 2) for mode 3.

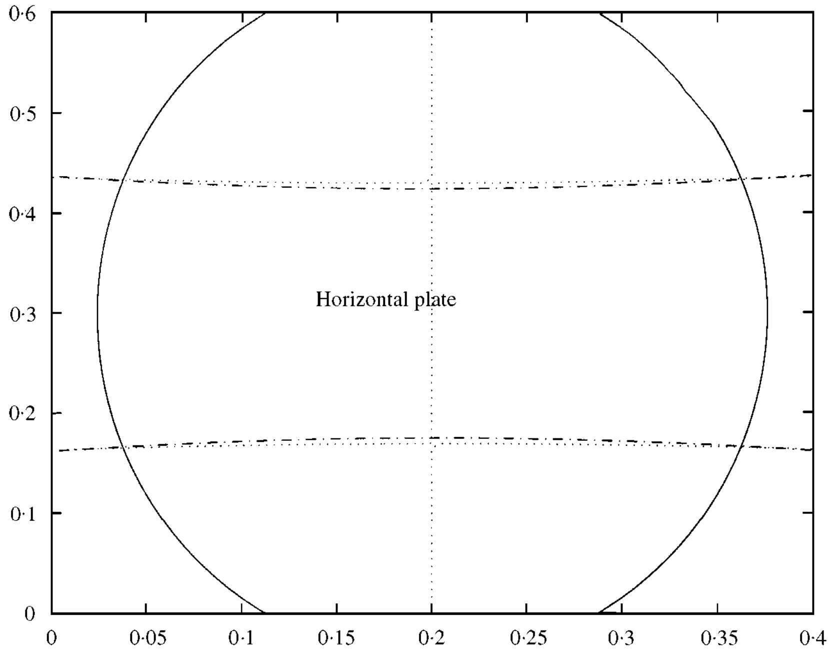

Figure 6. Null current density on the horizontal plate for modes 6 (—), 7 (.-.-) and 8 (.....).

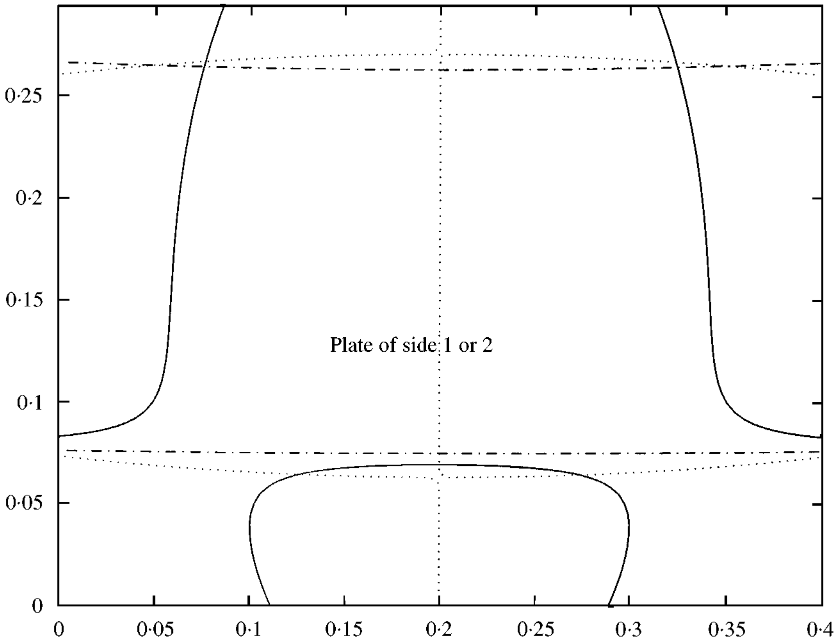

Figure 7. Null current density on the inclined plate (1 or 2) for modes 6 (—), 7 (.-.-) and 8 (.....).

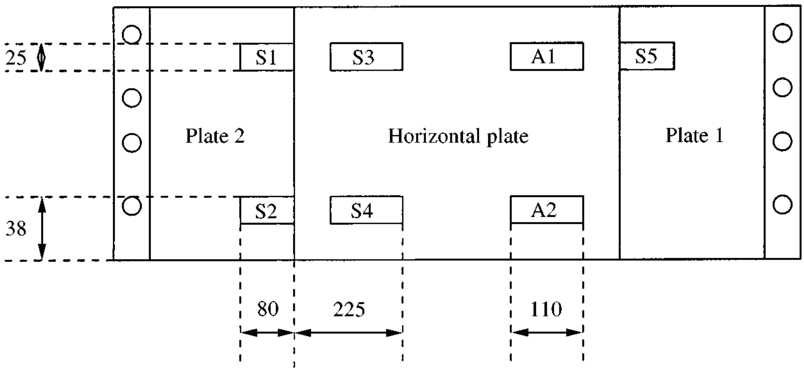

Figure 8. Optimized locations of PZT sensors and actuators on the structure (unit mm).

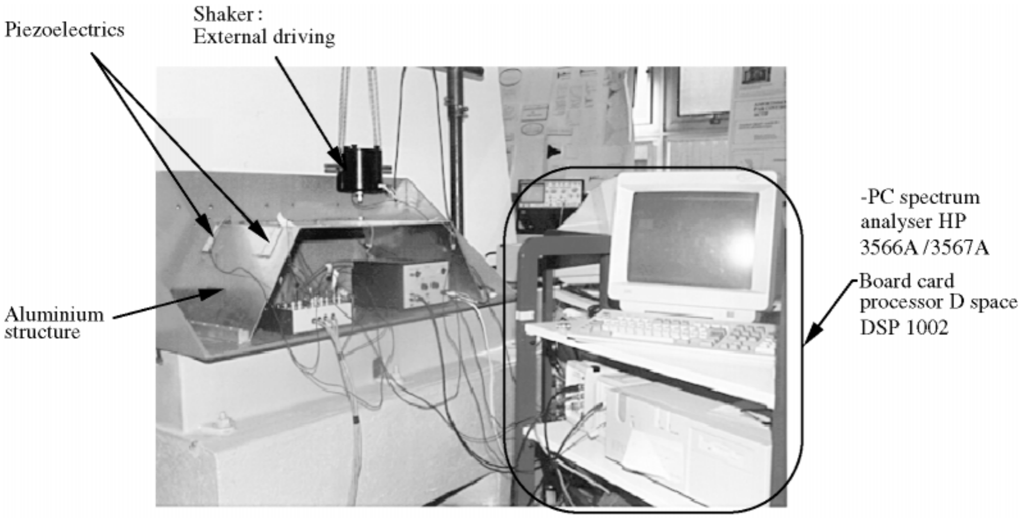

Figure 9. Photo of the experimental set-up.

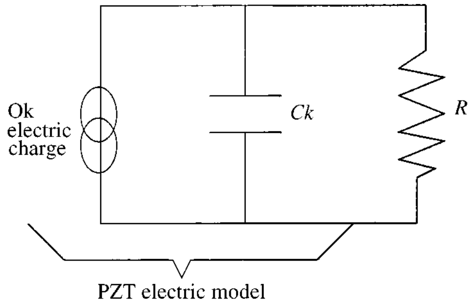

Figure 10. Model of PZT layer sensor.

V_k^s is the voltage picked up with DSP1002 and is related to the charge of the kth PZT sensor by

$$V_k^s = \frac{q_k}{C_k}\left(\frac{s}{s + \omega_k^0}\right), \tag{15}$$

where $\omega_k^0 = 1/RC_k$ and C_k is the kth PZT capacitance.

The cut-off frequency ω_k^0 of the high-pass filter, is approximately estimated in practice as (2π) (17·5 Hz) = 110 rad/s for each layer sensor. Since its value is located between the first- and the second-mode frequency, the real modal contributions of the first and second modes are not so easy to extract. To move the ω_k^0 value under the first-mode frequency (15 Hz) of the structure, we added in parallel with each PZT layer a capacity $C = 1$ μF to obtain $\omega_k^0 = (2p)$ (2·5 Hz) = 16 rad/s. Finally, to evaluate the accuracy of the numerical model, a comparison with the experimental measurements has been done. Figure 11 shows the superposition of theoretical and experimental transfer functions. One can note a little difference between the two plots. This can be justified by the small effects of the PZT layers on the modal shapes.

All the necessary parameters for the modal filters having been identified, two kinds of the IMSC control approaches were tested.

First, a brief description of modal displacements and velocities measurement is necessary. Three ways are possible.

The first consists of measuring both the current and the charge at the piezoelectric device electrodes. [See equation (9) for the current measurement by using a simple current amplifier as reported in reference [6] and equation (15) for the charge measurement using a capacitance in parallel with the piezoelectric sensor.) Then one can form two vectors of measurements $V_{current}^s$ and V_{charge}^s. Each of these two vectors gives the modal velocities or the modal displacements with the modal filter $K^s(1:5, 1:5)$.

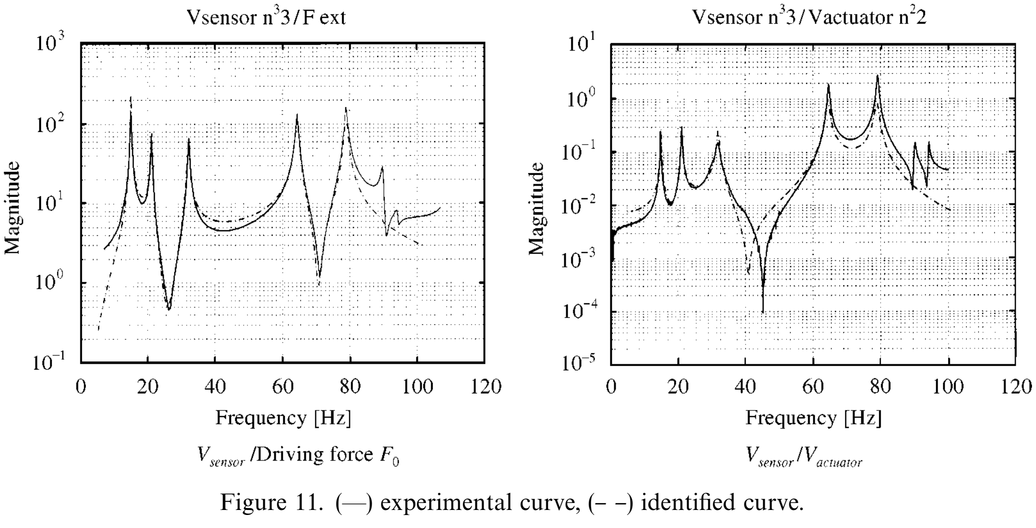

Figure 11. (—) experimental curve, (– –) identified curve.

The second way consists of using only the current measure ($V^s_{current}$) which gives only the modal velocities. The modal displacements are obtained by integrating the modal velocities.

The third method consists of using the charge measure (V^s_{charge}) which gives only the modal displacements. The modal velocities are obtained by differentiating the modal displacements.

The second method was used in the experimental set-up because we implemented only one kind of measure (current) and the integration was numerically more accurate and caused less errors than differentiating. The entire scheme of control is presented in Figure 12.

The first kind of IMSC control consists of controlling one mode. Figure 13 shows the result if one controls only the first mode at frequency 15 Hz. For the results when the other modes are controlled in the same way; see Figures 14–17. One can notice that the first mode is more difficult to control than the others because the horizontal plate where the actuators are glued is moving approximately as a rigid body. So, one needs much more energy to control this first mode.

The second kind of control consists of controlling in each step the mode with the highest energy level: this method is known as the time-sharing method. It also consists of controlling one single mode at a time. The difference between this and the *IMSC* control is the possibility to control all of the five modes during one test. At each time step, the *MIMSC* controller checks the amount of the modal energy of the five modes concerned, selects the mode with the highest energy and redirects the action to control it. One can note that the modal gains of the *MIMSC* controller are the same as those used for *IMSC* control. It is interesting because one does not need to use as many actuators as the number of modes to control and one does not need to use the pseudo-inverse of the actuation matrix as proposed by Lindberg [5]. However, the control command delivered is a kind of a discontinuous signal

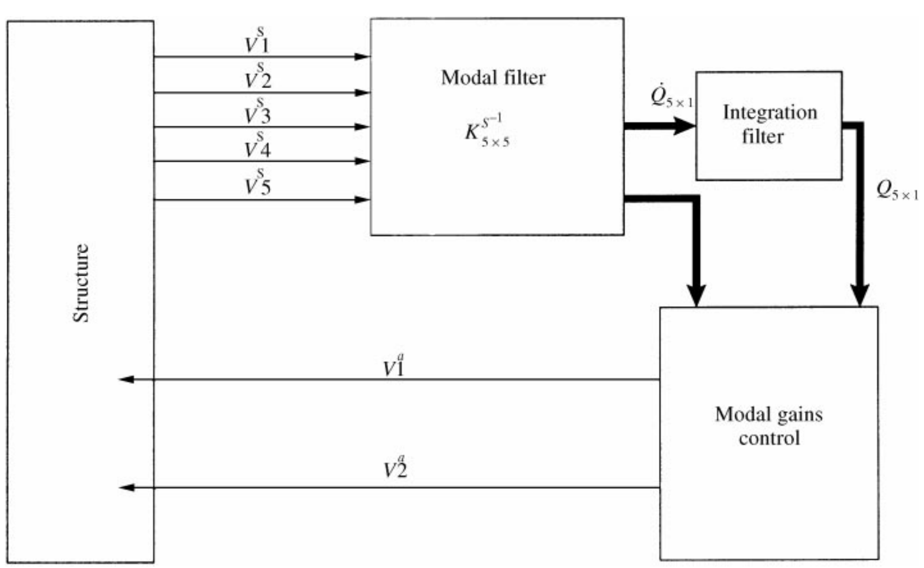

Figure 12. Modal control connections.

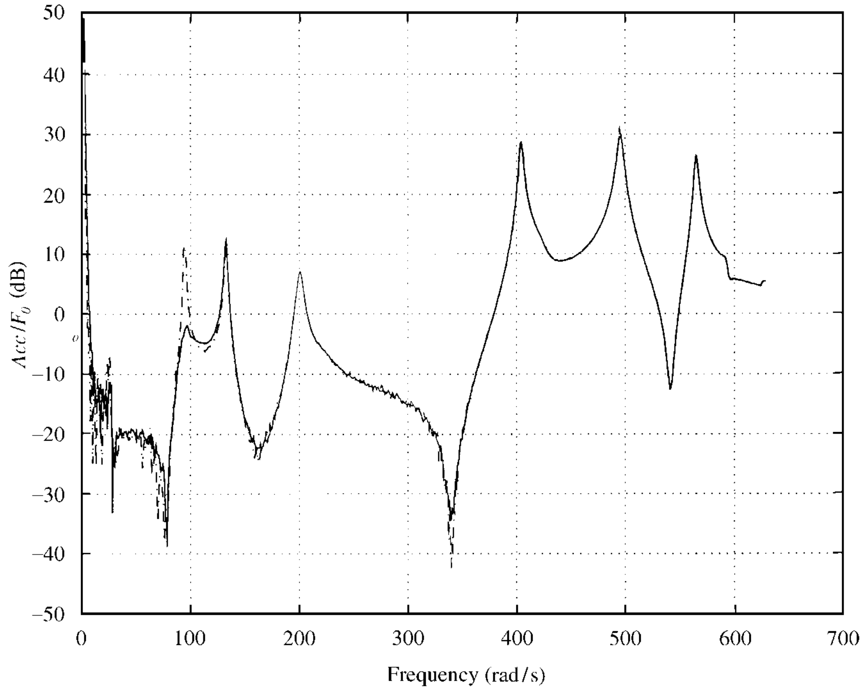

Figure 13. Modal control of one mode (mode 1). – · – · without control; — with control.

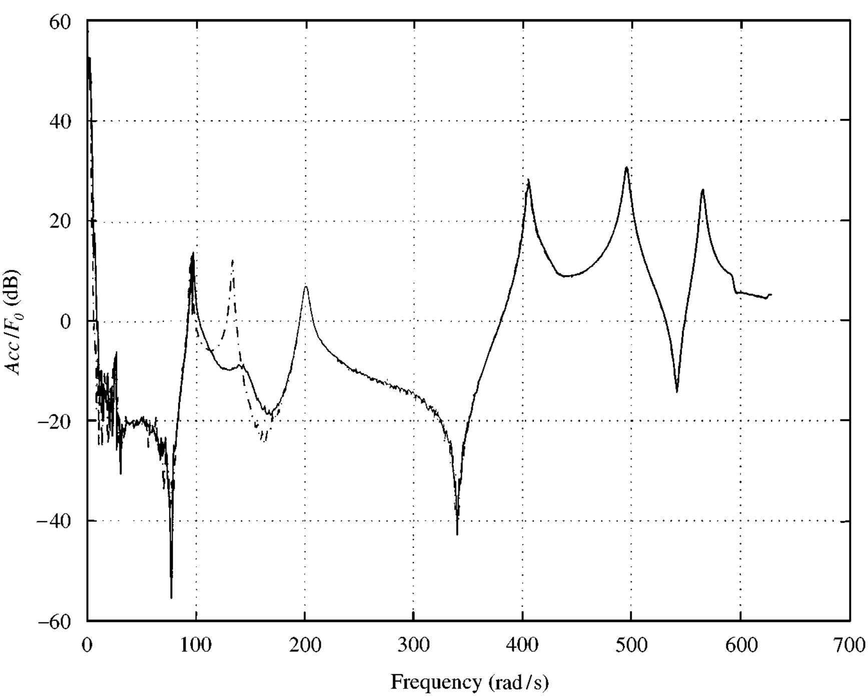

Figure 14. Modal control of one mode (mode 2). – · – · without control; — with control.

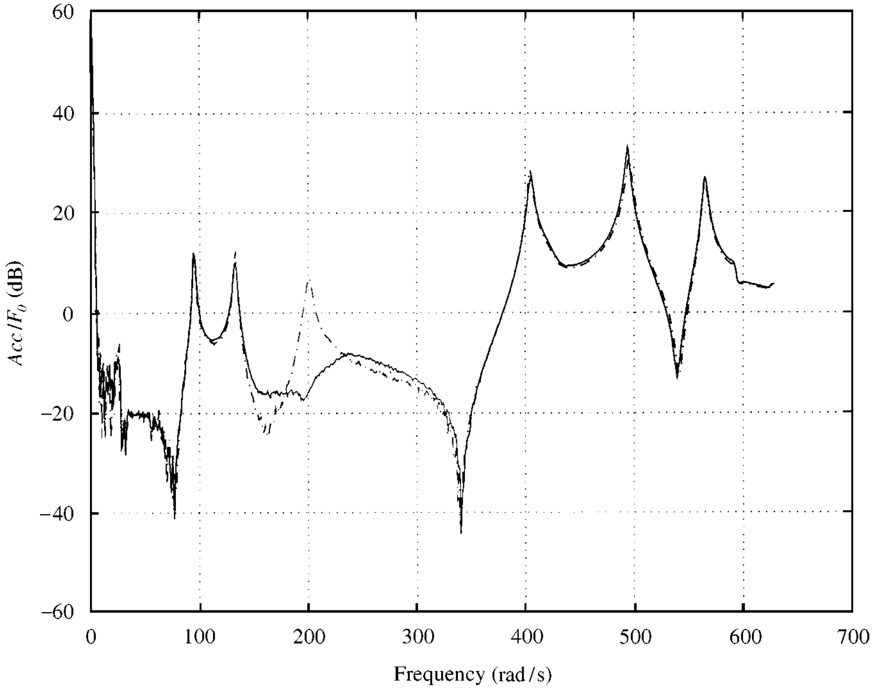

Figure 15. Modal control of one mode (mode 3). – · – · without control; — with control.

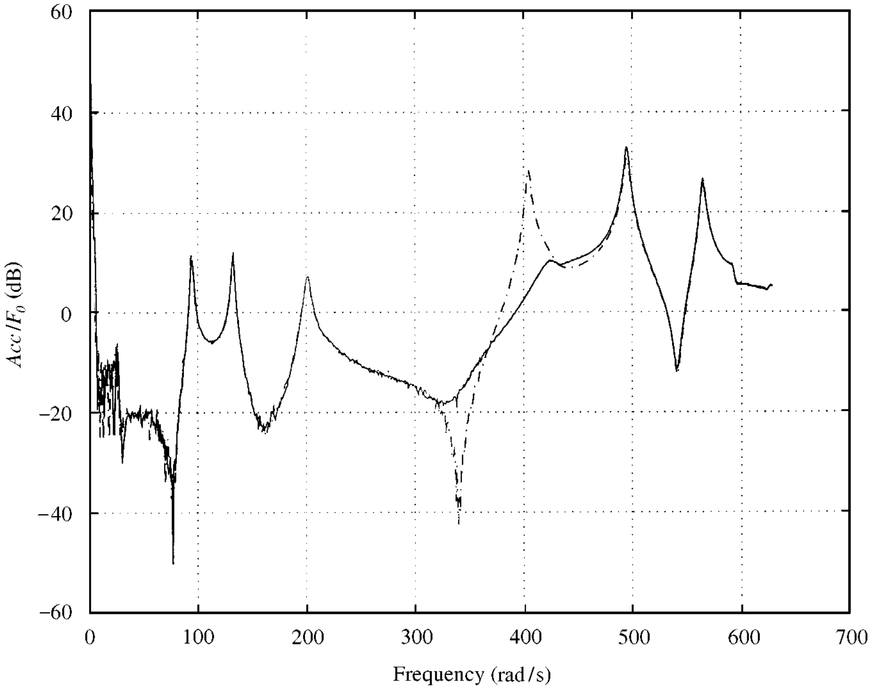

Figure 16. Modal control of one mode (mode 4). – · – · without control; — with control.

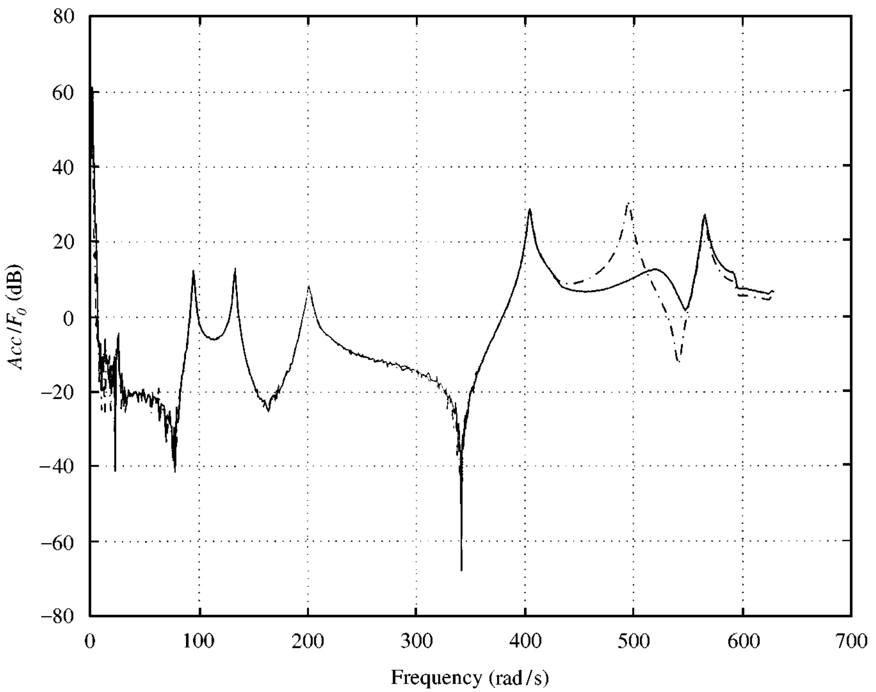

Figure 17. Modal control of one mode (mode 5). – · – · without control; — with control.

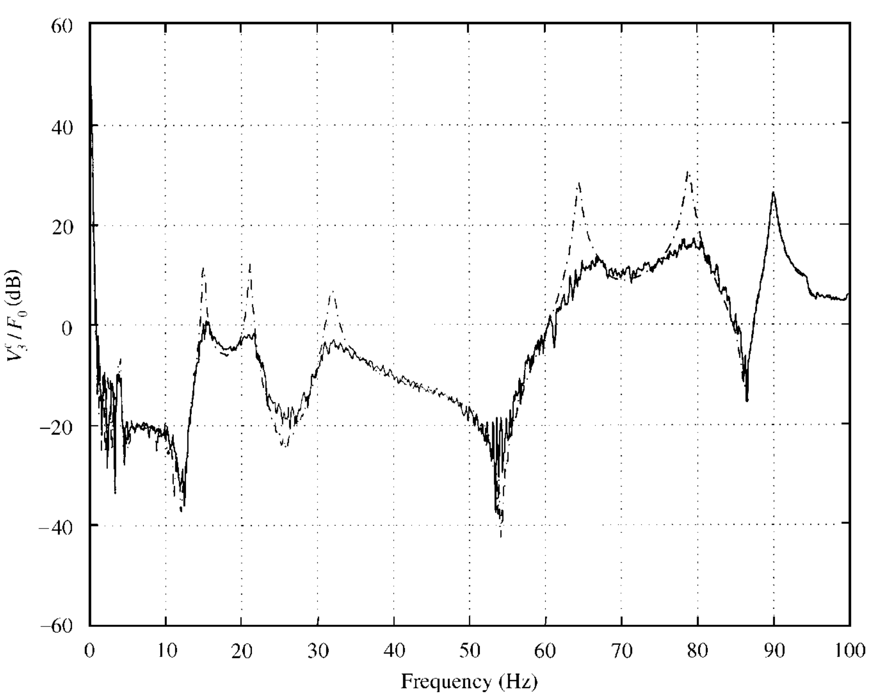

Figure 18. Modal control with time-sharing (*MIMSC*). – · – · without control; — with control.

TABLE 1

Control performances

Mode No.	1	2	3	4	5
Measured frequency	15	21·2	32	64·4	78·9
Control gain R	5e-4	5e-4	1e-3	1e-3	1e-3
ξ_0 modal (%)	0·51	0·59	0·75	0·45	0·38
Modal gain (dB)	14	21	22	23	20
Gain $MIMSC$	14	15	10	20	15
$\xi_{control}/\xi_0$ modal	5	11·9	12·6	14	10
$\xi_{control}/\xi_0$ $MIMSC$	5	5·6	3	10	3

which may cause instability. So we proceeded to smooth out the control signal. Figure 18 shows the performance of such a control.

Table 1 shows, the values of the damping ratios ξ. This is because the control command is dominated by a term proportional to the modal velocity. So the control is in fact an active damping. Determination and comparison between modal damping of the controlled structure and the non-controlled structure is a way to see the efficiency of the modal control. One can note easily that the modal gain of the first mode is less than for the others. The gains of the third and the fifth modes are also less than the others because the associated eigenfunctions are asymmetric and then more difficult than the symmetric ones to excite with the actuators.

6. CONCLUSION

In this paper, we have presented the modal control strategy and an optimization method for actuator and sensor locations. In modal control, one needs to extract modal variables and to minimize the spillover effect. The optimization of location is then a fundamental step to construct a modal filter that extracts the modal velocities of the controlled modes and minimizes the modal variables of the unwanted modes. An optimized actuator location will reduce the spillover phenomena. In the experimental study a complex structure is used. We performed two methods of control that need fewer actuators than modes to control. Indeed, both methods consist of controlling one mode at each step. In the first one, one mode is controlled all the time, but in the second, the mode with the highest energy level is controlled at each step (*MIMSC* or Time-Sharing). The two methods are efficient and robust (the modal gains are 10–20 dB) but it will be more interesting to control more than five modes using only the five sensors and ensure the same performances and robustness. This problem will be treated by using an LQG scheme with or without a Kalman filter.

REFERENCES

1. L. MEIROVICH and H. BARUH 1981 Control of self adjoint distributed parameters systems. *AIAA Guidance and Control* **5**, 60–66.

2. L. Meirovich and H. Baruh 1982 *Journal of Guidance* 6. Robustness of the independent modal space control.
3. L. Meirovich, H. Baruh and O. Öz 1982 *Journal of Guidance* 4. A comparison of control techniques for large flexible structures.
4. L. Meirovich 1989 *Dynamic and Control of Structures*. New York: Wiley.
5. R. E. Lindberg (1984) *Journal of Guidance* 7(2), On the number and placement of actuators for independent modal space control.
6. C. K. Lee 1990 *Journal of Acoustical Society of America* **3**, 87. Theory of laminated piezoelectric plates for the design of distributed sensors/actuators. Part I: governing equations and reciprocal relationships.
7. A. Hac and L. Liu 1993 *Journal of Sound and Vibration* **2**, 239–261. Sensors and actuators location in motion control of flexible structures.
8. M. Collet and L. Jezequl (1994) *Journal of Structural Control* **1**, Active modal control with piezoelectric layers optimisation.